Composites Communications 35 (2022) 101315

Contents lists available at ScienceDirect

Composites Communications

journal homepage: www.elsevier.com/locate/coco

Advanced microscopic characterisation of multi-scale high-resolution mechanical behaviour of a nacre-inspired composite

Jingyi Mo [a], Nathanael Leung [a], Urangua Jargalsaikhan [a], Hongbo Wan [a,b], Bin Zhu [a], Bo Su [b], Tan Sui [a,*]

[a] School of Mechanical Engineering, University of Surrey, UK
[b] Biomaterials Engineering Group (bioMEG), Bristol Dental School, University of Bristol, UK

ARTICLE INFO

Keywords:
Nano-indentation
Residual stress
Bioinspired composite
Mechanical properties

ABSTRACT

A nacre-inspired composite with a lamellar architecture of polymethyl methacrylate (soft and tough phase) and alumina (stiff phase) was fabricated using a bidirectional freezing casting technique. The bulk fracture mechanics of the nacre-inspired composite has been reported along with detailed microstructural analysis. The mechanistic connection between microstructure and mechanical properties at the micro- and macro-scale was not fully understood. Herein we addressed this issue by quantifying phase-specific hardness, modulus, and residual stress at the micro-scale level and compared with the bulk mechanical response. A shear-lag model was applied to provide a quantitative understanding of the softening effects resulting from residual stress and the microstructure. Our findings demonstrated the potential of bioinspired synthetic architectures in providing a tuneable model system to investigate the underlying design principles of more complex hierarchical biological materials.

1. Introduction

Good mechanical properties such as Young's modulus, strength and fracture toughness are antagonistic combinations that are usually not readily achieved in engineered materials. Nevertheless, some natural materials, like nacre, exhibit a remarkable combination of both high strength and toughness by employing a unique hierarchical architecture and complicated physical and chemical interactions at different length scales. Multiple fabrication techniques, such as replicating, direct foaming, sacrificial templating, and 3D printing, have been developed for bioinspired manufacturing [1,2]. However, these techniques have several limitations, e.g., they are often time-consuming or size-limiting, not environmentally friendly, too costly, or cannot provide precise control over the microstructure.

Recently, a cost-effective bidirectional freezing-casting technique has been developed, which can assemble small building blocks (ceramic particles, platelets, and/or polymer) into a large-sized (centimetre-scale) lamellar architecture akin to natural nacre [3]. By controlling the fabrication parameters, such as freezing conditions, densification, and different combinations of ceramics (hard phase) and polymers or metals (soft phase), the microstructure and mechanical properties of the bio-inspired composites can be tuned and enhanced [4,5]. Micromechanical testing has been used to understand the interfacial bonding that contributes to nacre's high toughness and the replication and optimisation of this feature in freeze-casted composites [6,7]. Further understanding of the phase-specific mechanical response at multiple length scales is critical for achieving the fundamental insight as well as the broader application of the novel bioinspired composites.

Herein, an extended nano-indentation technique was used to evaluate the microhardness and micromodulus of the bioinspired composite. It was also used to analyse the micro-scale phase-specific residual stress by comparing the load level of the stressed surface to the stress-free surface of a micro-pillar, which provides insight of the crack initiation and propagation in the nacre-inspired composite, as visualised by *in situ* SEM micromechanical testing. Such a novel analytical approach could help build a detailed mechanistic correlation between micro-scale residual stress and macro-scale modulus; and address the issues related to the structural integrity arising from residual stress, which could also be used for the optimisation of the fabrication processing.

* Corresponding author.
E-mail address: t.sui@surrey.ac.uk (T. Sui).

https://doi.org/10.1016/j.coco.2022.101315
Received 27 July 2022; Received in revised form 1 September 2022; Accepted 4 September 2022
Available online 8 September 2022

2. Materials and methods

2.1. Sample preparation

The fabrication method used to prepare the nacre-inspired alumina (Al_2O_3)/poly(methyl methacrylate) (PMMA) composite was reported in detail in Ref. [8].

2.2. Microstructural characterisation

The composite sample was firstly polished using a series of resin-bonded diamond surfaces (Struers, Copenhagen, Denmark) in ascending grit order on an automatic polisher. The microstructure of the Al_2O_3/PMMA composite was characterised using a Jeol-7100F SEM (Tokyo, Japan). Analytical SEM-EDS mapping was performed on the stress-free ring-core over a 50 × 40 μm^2 region of interest (ROI) using an UltraDry EDS detector (Thermo Fisher Scientific, Massachusetts, United States). The distribution map of Al and C were obtained from the ROI by

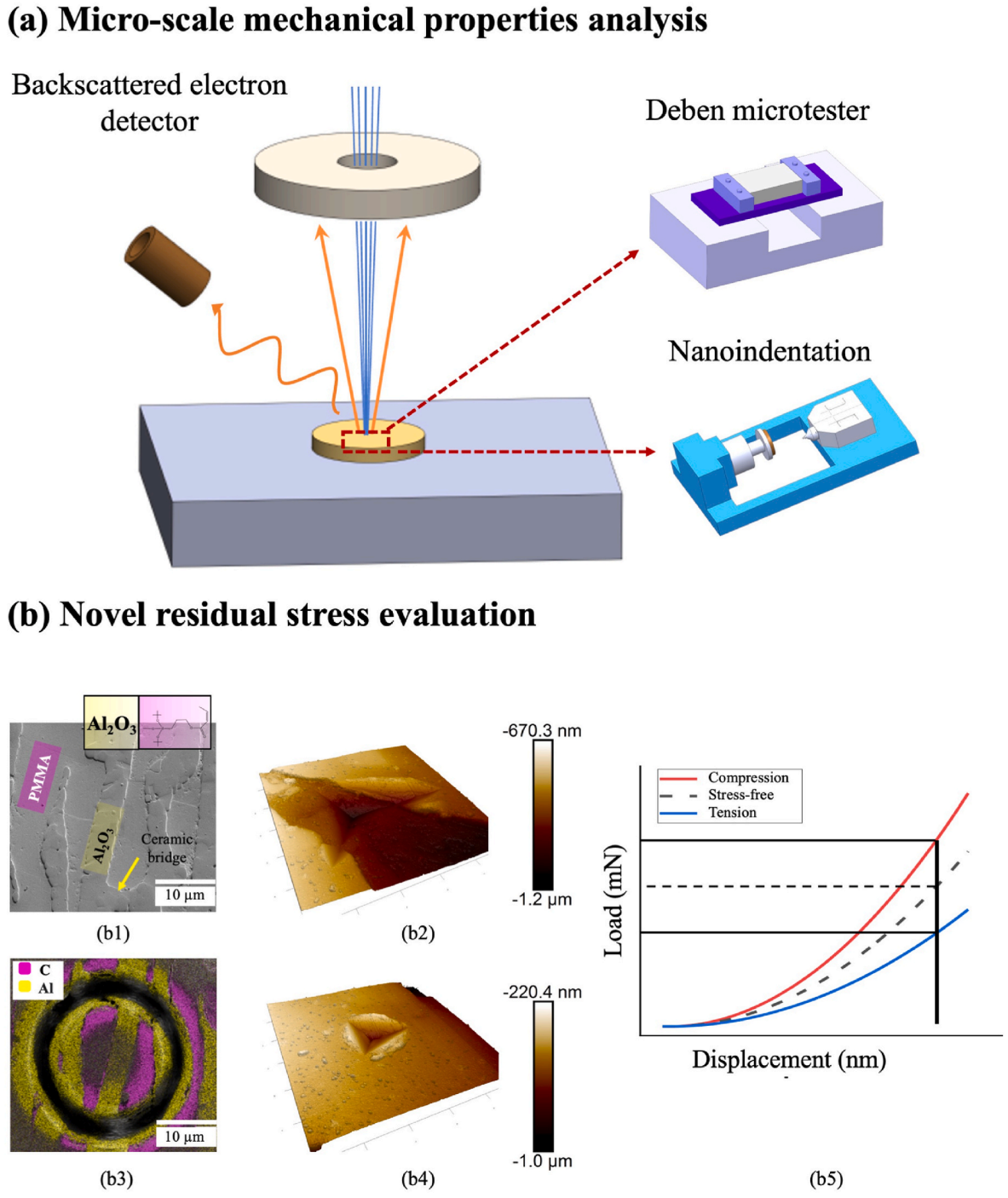

Fig. 1. (a) Experimental set-up of the *in situ* SEM micromechanical testing and the extended nano-indentation. (b1) SEM images showing the lamellar structure of the nacre-inspired composites, the internal residual stress remained balanced with the presents of compressed and tensile stress. (b2, b4) AFM images of the nano-indentation imprints on Al_2O_3 and PMMA. (b3) EDS spectra of stress-free micro-pillar. (b5) Load-displacement curves of the nano-indentation testing on the surface under compression, tension and stress-free states.

analysing each element's weight percentage from the EDS spectra using Pathfinder™ software.

2.3. Micro-scale mechanical properties analysis and novel residual stress evaluation

The nano-indentation experiments were carried out on a cross-sectioned surface of the Al_2O_3/PMMA nacre-mimetic composite ((Fig. 1 (b1)) using an ASA nano-indentation stage (Alemnis, Thun, Switzerland) with a Berkovich indenter tip. Displacement-controlled indentations were performed to a depth of 300 nm with a loading rate of 10 nm/s, and the micro-mechanical properties, including hardness (H) and Young's modulus (E), were determined using Oliver–Pharr method [9,10]. A matrix of 6 × 6 indentations with a spacing of 6 μm was performed.

The micro-scale ring-core Xe^+ plasma focused ion beam (PFIB) milling was applied to obtain a residual stress-free sample which will then serve as the reference sample for calculating the residual stress [11]. Herein, three micro-scale ring-cores with a diameter of 25 μm were milled with a beam energy of 30 keV and beam current of 10 nA (Fig. 1 (b3)). The final milling depth of the ring-core is 25 μm as it needs to be equal to the diameter of the ring-core to achieve full stress relief. Four indents were executed on each stress-free ring-core with the same experimental parameters as performing the 6 × 6 nano-indentation matrix on the same material with residual stress. The residual stress was determined by comparing the load-depth curve and contact area differences between the stress-free reference sample with the same sample having residual stress (Fig. 1(b5). The value of residual stress was derived using the following equation [12]:

$$\sigma_R = \frac{3(L_0 - L)}{2A_C} \quad (1)$$

2.4. Bulk mechanical properties analysis: in situ SEM mechanical testing

The *in situ* compression mechanical testing was conducted with a Deben mechanical microtester (Suffolk, UK) inside a MIRA II SEM (TESCAN, Brno, Czech Republic), as shown in Fig. 1 (a). The composite specimens (2.5 × 2.5 × 3.5 mm^3) were tested with a loading rate of 0.1 mm/min. The load-displacement data and the imaging video were synchronised and recorded during the compression test.

3. Results and discussions

3.1. Microstructural characterisation

EDS analysis was performed on the micro-pillar (Fig. 1 (b3)) which showed the distinct multi-layered architecture of the composite with the Al_2O_3 and PMMA phases highlighted in yellow and pink, respectively. The mean thickness of Al_2O_3 lamellae obtained from the image-based analysis method was found to be 7.7 ± 2.1 μm.

3.2. Micro-scale mechanical behaviour by nano-indentation

An SEM image of the nano-indentation map was superimposed with the modulus and hardness maps as shown in Fig. 2 (a, b, d, e). The hardness and modulus in the PMMA layer were lower than those in the Al_2O_3 layer, validating the hard-soft lamellar architecture in our nacre-inspired composite.

The micro-scale residual stress in the Al_2O_3 or PMMA led to changes in measured hardness and modulus (Fig. 2 (a, b, d, e)). Stressed Al_2O_3 (99.2 ± 14.5 GPa) had a ~40% higher modulus compared to the stress-free counterparts (68.9 ± 13.1 GPa), whereas the modulus of PMMA (5.0 ± 0.6 GPa) was ~8% lower than the stress-free counterparts (5.4 ± 0.7 GPa). Fig. 2 (b, e) showed the hardness of stressed and stress-free states for the two phases, which is observed to be consistent with Fig. 2 (a, d), indicating that stressed Al_2O_3 had a hardness of 7.8 ± 1.4 GPa, larger than stress-free samples (5.5 ± 1.7 GPa), whereas stressed PMMA (0.3 ± 0.03) was two times higher compared with the stress-free samples (0.9 ± 0.2 GPa).

The observed difference in the modulus and hardness of the individual constituent phases in both as-fabricated and PFIB milled samples were conceived in light of an important experimental finding, that is internal residual stresses as revealed by nano-indentation tests. An important contributor to nacre's excellent fracture toughness properties is a high interfacial bonding strength between the bioceramic and biopolymer phases [6]. With the modification of ceramic surface salinisation during the manufacturing process, it is possible to emulate the high interfacial strength between the ceramic and polymer phases,

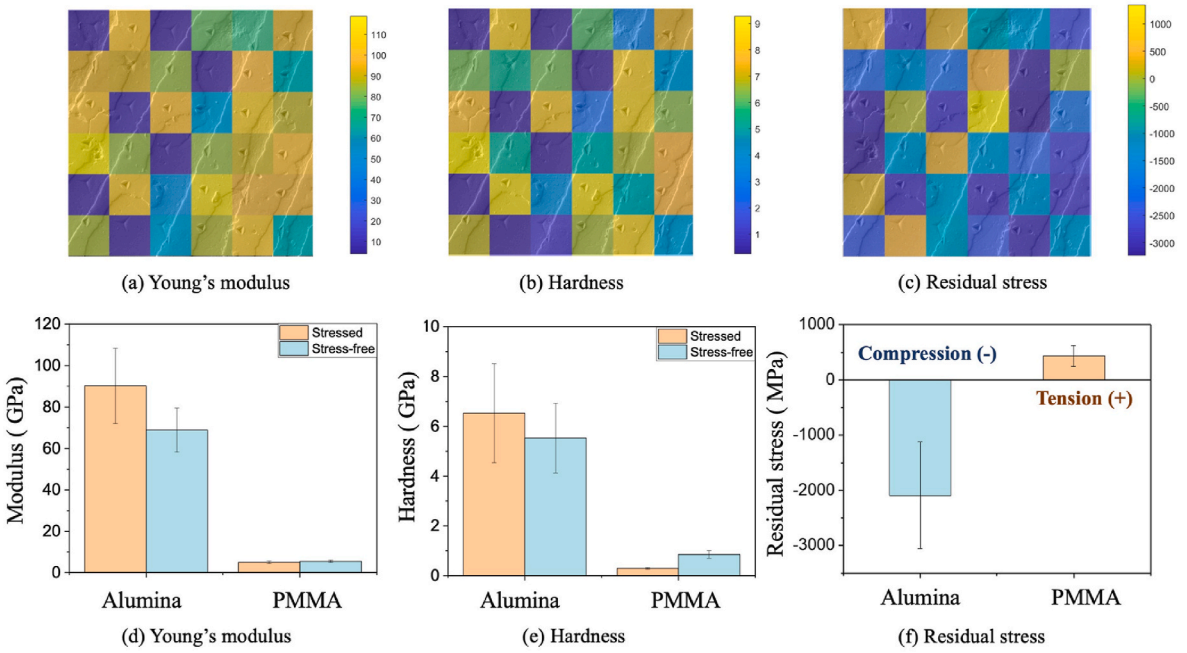

Fig. 2. SEM images of the nano-indentation imprints and the corresponding Young's modulus (a, d), hardness (b, e), and residual stress maps (c, f).

which was found to have a profound impact on the toughness of freeze-casted composites [7]. However, the formed covalent bonding between the phases has the potential to introduce residual stresses within the individual phases. During manufacturing, the PMMA shrunk during the polymerisation of the MMA monomers. The contraction of the polymer phase was constrained by the covalent bonds with the ceramic via the silane coupling agent, which inevitably led to the development of residual stress in the composite both at the ceramic-polymer interface and within each individual constituent. Consequently, the ceramic phase was stressed in compression whilst the polymer was stressed in tension. When a nano-indentation test was attained in a stress-free surface, and if compressive stress was applied to the surface with a fixed displacement, the measured load would increase to a higher level due to the increased surface penetration resistance, as shown in Fig. 1 (b2). This would be the opposite for tensile residual stress. Calculation based on the theory proposed by Lee and Kwon [12] (Eq. (1)) showed indeed that high residual stresses were stored in the as-fabricated nacre-inspired composite.

Quantitative analysis of the residual stress distribution on the surface of the nacre-inspired composite is shown in Fig. 2 (c, f). As expected, the PMMA experienced an in-plane biaxial tensile stress, whilst the Al_2O_3 underwent in-plane biaxial compressive stress due to the polymer shrinkage in the manufacturing process. The maximum compressive residual stress had the greatest value of −3.2 GPa at the interfacial region between the Al_2O_3 and PMMA layer. The mean value of the residual stress for Al_2O_3 and PMMA were −2.1 ± 0.9 GPa and 0.4 ± 0.2 GPa, respectively. The presence of residual stress, especially the compressive stress in the Al_2O_3 phase, is generally favourable for the mechanical performance of ceramic/polymer composites since this stress can augment the pull-out energy dissipation of the Al_2O_3 by closing initial microcracks and facilitating crack deflection. In contrast, the formation of tensile residual stress may be detrimental in the production of ceramic/polymer composite, for instance, positive residual stress in the polymer phase may lead to interface debonding or micro-cracking. Such initial material damage may serve as sites where the environmental degradation or nucleation of microcracks initiate. The structural integrity of the nacre-inspired composite is controlled by these internal stresses. Thus, any experimental studies assessing fracture mechanics of composite materials should consider the role that residual stress plays if they exist.

Considering this, the residual stress in the nacre-inspired composite can be determined based on the differences of measured load and contact area at the same penetration depth for stress-free and residually stressed samples (Eq. (1)) [12,13]. However, the load and depth curve for a stress-free sample is often not available, especially for those samples with complex preparation procedures. Here, the existing limits for residual stress determination had been overcome by performing the nano-indentation tests on a stress-free micro-pillar as shown in Fig. 1 (b3), where the residual stress had been fully relieved after incremental PFIB milling.

3.3. Bulk mechanical properties

The compressive engineering stress-strain curve of the Al_2O_3/PMMA composite is shown in Fig. 3(a). The tested nacre-inspired composite samples can still carry a load beyond the yielding point. The composite showed a yield strength of 293.4 ± 11.4 MPa, and an ultimate compressive strength of 309.5 ± 7.8 MPa with a total compressive strain of 5.3 ± 0.9% before failure. The modulus of this composite, as measured by the slope of the linear part of the loading curves, was 10.6 ± 1.1 GPa. We estimated from the conventional rule-of-mixtures (RoM) that the modulus of the nacre-inspired composite was in the range of 16.1–51.1 GPa, which seemed a little higher compared to the experimentally determined value (10.6 ± 1.1 GPa).

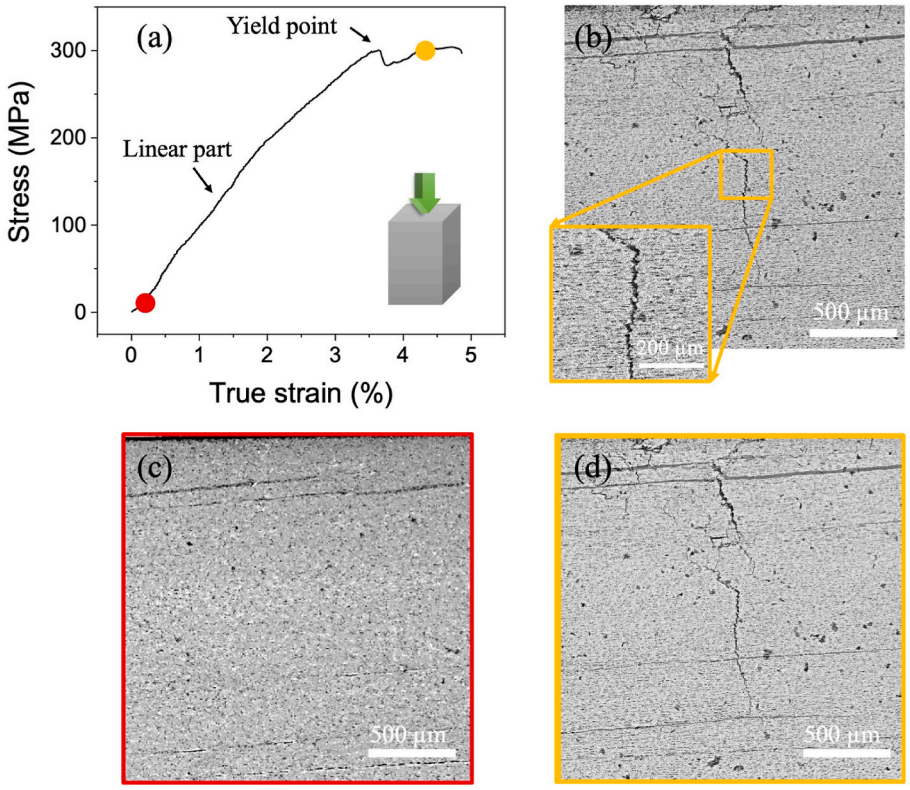

Fig. 3. (a) Engineering stress-strain curve of the Al_2O_3/PMMA composite obtained from *in situ* SEM micro-mechanical testing. (b) SEM images taken after failure showing the crack propagation behavior of Al_2O_3/PMMA composite. (c, d) SEM images taken during deformation, scanned points are indicated in red and yellow. (For interpretation of the references to colour in this figure legend, the reader is referred to the Web version of this article.)

3.4. Correlation between residual stress, microstructure, and microhardness

The effects of residual stress on the bulk mechanical properties at room/elevated temperature and fatigue life had been studied extensively [14–16]. However, to the best of our knowledge, no explanation had been given to the effects of the residual stresses on the macroscopic mechanical properties before the occurrence of microdamage. Shi et al. showed how the residual stresses affected the Young's modulus of cantilever beams [17]. Reynaud et al. demonstrated that the averaged tensile elastic modulus of SiC/SiC ceramic-matrix composites reached the value of the compressive mean elastic modulus when residual thermal stresses were relieved under fatigue testing. However, a direct explanation was not provided [15].

To establish the effect of residual stress on the mechanical performance of the nacre-inspired composite in this work, we interpreted our stress-strain data with an adapted shear-lag model proposed by Jackson et al. [18] and others for the deformation of nacre, tendon, enamel and dentine [19–22]. For the nacre-inspired composite, the SEM images of the fracture surface showed typical pull-out behaviour of the Al_2O_3 lamellae after failure, which suggested that pull-out was the predominant energy dissipation mechanism (Fig. 3 (b)). Based on these experimental observations, using the RoM, the shear lag model predicts the composite modulus under pull-out mode as follows:

$$E_c = \alpha E_l f_l + E_m(1 - f_l) \quad \text{Eq. 2}$$

where α is a stress transfer efficiency term, f_l is the volume fraction of Al_2O_3 lamellae, and E_l and E_m are the lamellae modulus and matrix modulus, respectively. The stress transfer term α depends on the fracture behavior of the composite. For the composite

$$\alpha = \frac{\tau S}{2E_l} \quad \text{Eq. 3}$$

which results in the simplified relationship:

$$E_c = \frac{\tau_{eff} S f_l}{2} + E_m(1 - f_l) \quad \text{Eq. 4}$$

where τ_{eff} is the shear modulus of the lamellae-matrix interface and S is the aspect ratio of the lamellae.

The stress transfer efficiency term α for natural nacre and other mineralised biological materials can be estimated by Ref. [23]:

$$\frac{1}{\alpha} = 1 + \frac{1}{S^2}\frac{1 - f_l}{f_l}\frac{E_l}{\gamma_{mE_m}} \quad \text{Eq. 5}$$

Where $\gamma_m \sim 0.36$ is the ratio between shear (G_m) and Young's modulus (E_m) of the matrix ($G_m = \gamma_{mE_m}$). From the SEM analysis, the aspect ratio (S) of the Al_2O_3 lamellae is estimated to be ~325. Since the second term on the right-hand side is in the order of 0.0001, we can neglect this term in Eq. (5), leading to $\alpha \sim 1$.

Using this value for S in Eq. (3) along with the estimate of the stress transfer efficiency $\alpha \sim 1$, an estimate for τ can be obtained, $\frac{\tau S}{2E_l} \sim 1$, which was found to be ~0.2 GPa. The effect of residual stress, μ, on E_c can be estimated by substituting an effective modulus, $\tau_{eff} = \tau - \mu$:

$$E_c = \frac{S f_l}{2}(\tau - \mu) + E_m(1 - f_l) \quad \text{Eq. 6}$$

After the estimates for E_m and S are obtained, we can now use this equation to evaluate the effects of residual stress on the overall mechanical performance of the nacre-inspired composite. It is estimated that the shear modulus of the interface between Al_2O_3 lamellae and PMMA (μ) is reduced by 0.128 GPa due to the presence of residual stress. The reduced modulus of the composite determined by the experiment is possibly due to the mechanical discontinuities in the composite, e.g., micro-pores, which might act as a weak point leading to crack initiation and propagation during mechanical loading. A detrimental role is played by tensile residual stress with peak stress distributed at the interface of the Al_2O_3 lamellae and PMMA phase. In this case, the modulus of the nacre-inspired composite is reduced due to a lower stress transfer and load-bearing capacity shear modulus at the Al_2O_3 lamellae and PMMA interface. The reasonable agreement between the experimentally determined values and the stress level expected from these calculations suggests that residual stresses are likely the reason for the lower maximum composite modulus compared with the theoretical prediction.

4. Conclusions

In summary, the use of novel combined methods for mechanical parameter evaluation at multiple length scales in the micro-scale composite system enabled us to quantify both the materials-level mechanism and phase-specific contribution of the nacre-inspired composite with the presence of preexisting residual stresses. Phase specific residual stress analysis demonstrated that the Al_2O_3 phase was under compression whilst the PMMA phase experienced tension. The reduction of stresses transferred at the micro-scale directly translated into reduced composite modulus at the macro-scale. The presence of tensile residual stress in the PMMA phase led to an approximately 36% reduction in shear modulus at the ceramic lamellae-polymer interface, underpinning the reduced bulk Young's modulus measured by experimentation compared to the RoM model prediction. A shear-lag model was applied to provide quantitative understanding of the softening effects caused by residual stress and microstructure. Our work on the nacre-inspired composite demonstrated the potential of bioinspired synthetic architectures in providing a tuneable model system to investigate the underlying design principles of more complex hierarchical biological materials.

CRediT authorship contribution statement

Jingyi Mo: Data curation, Methodology, Formal analysis, Investigation, Writing – original draft, Visualization. **Nathanael Leung:** Formal analysis, Methodology, Writing – review & editing. **Urangua Jargalsaikhan:** Writing – review & editing, Visualization. **Hongbo Wan:** Methodology, Investigation. **Bin Zhu:** Methodology, Investigation. **Bo Su:** Validation, Investigation, Resources, Writing – review & editing, Visualization, Supervision. **Tan Sui:** Conceptualization, Methodology, Formal analysis, Investigation, Resources, Writing – original draft, Supervision, Funding acquisition.

Declaration of competing interest

The authors declare that they have no known competing financial interests or personal relationships that could have appeared to influence the work reported in this paper.

Data availability

Data will be made available on request.

Acknowledgements

This work was supported by the Engineering and Physical Sciences Research Council (EPSRC) project (EP/S022813/1).

References

[1] T. Ohji, M. Fukushima, Macro-porous ceramics: processing and properties, Int. Mater. Rev. 57 (2012) 115–131, https://doi.org/10.1179/1743280411Y.0000000006.

[2] A.R. Studart, U.T. Gonzenbach, E. Tervoort, L.J. Gauckler, Processing Routes to Macroporous Ceramics: A Review, Journal of the American Ceramic Society, 2006, https://doi.org/10.1111/j.1551-2916.2006.01044.x.

[3] Q. Cheng, C. Huang, A.P. Tomsia, Freeze casting for assembling bioinspired structural materials, Adv. Mater. 29 (2017), 1703155, https://doi.org/10.1002/adma.201703155.
[4] Q. Cheng, L. Jiang, Z. Tang, Bioinspired layered materials with superior mechanical performance, Acc. Chem. Res. 47 (2014) 1256–1266, https://doi.org/10.1021/ar400279t.
[5] J. Wang, Q. Cheng, Z. Tang, Layered nanocomposites inspired by the structure and mechanical properties of nacre, Chem. Soc. Rev. 41 (2012) 1111–1129, https://doi.org/10.1039/C1CS15106A.
[6] J. Liu, Y. Xu, H. Yang, Y. Liu, P.K.D.V. Yarlagadda, C. Yan, Investigation of failure mechanisms of nacre at macro and nano scales, J. Mech. Behav. Biomed. Mater. 112 (2020), 104018, https://doi.org/10.1016/j.jmbbm.2020.104018.
[7] J. Liu, R. Bai, Z. Lei, C. Xu, Q. Ye, W. Martens, P.K. Yarlagadda, C. Yan, Experimental and numerical investigation of the toughening mechanisms in bioinspired composites prepared by freeze casting, Compos. Sci. Technol. 182 (2019), 107768, https://doi.org/10.1016/j.compscitech.2019.107768.
[8] H. Wan, N. Leung, S. Algharaibeh, T. Sui, Q. Liu, H.X. Peng, B. Su, Cost-effective fabrication of bio-inspired nacre-like composite materials with high strength and toughness, Compos. B Eng. 202 (2020), 108414, https://doi.org/10.1016/j.compositesb.2020.108414.
[9] W.C. Oliver, G.M. Pharr, An improved technique for determining hardness and elastic modulus using load and displacement sensing indentation experiments, J. Mater. Res. 7 (1992) 1564–1583, https://doi.org/10.1557/JMR.1992.1564.
[10] W.C. Oliver, G.M. Pharr, Measurement of hardness and elastic modulus by instrumented indentation: advances in understanding and refinements to methodology, J. Mater. Res. 19 (2004) 3, https://doi.org/10.1557/jmr.2004.19.1.3.
[11] B. Zhu, Y. Wang, J. Dluhoš, A.J. London, M. Gorley, M.J. Whiting, T. Sui, A novel pathway for multiscale high-resolution time-resolved residual stress evaluation of laser-welded Eurofer97, Sci. Adv. 8 (2022), https://doi.org/10.1126/sciadv.abl4592 eabl4592.
[12] Y.-H. Lee, D. Kwon, Measurement of residual-stress effect by nanoindentation on elastically strained (100) W, Scripta Mater. 49 (2003) 459–465, https://doi.org/10.1016/S1359-6462(03)00290-2.
[13] C.A. Charitidis, D.A. Dragatogiannis, E.P. Koumoulos, I.A. Kartsonakis, Residual stress and deformation mechanism of friction stir welded aluminum alloys by nanoindentation, Mater. Sci. Eng. 540 (2012) 226–234, https://doi.org/10.1016/j.msea.2012.01.129.
[14] A.G. Evans, F.W. Zok, R.M. McMeeking, Fatigue of ceramic matrix composites, Acta Metall. Mater. 43 (1995) 859–875, https://doi.org/10.1016/0956-7151(94)00304-Z.
[15] G. Fang, X. Gao, G. Yu, S. Zhang, J. Chen, Y. Song, Effect of the stress level on the fatigue strengthening behavior of 2D needled C/SiC CMCs at room temperature, Mater. Des. 89 (2016) 432–438, https://doi.org/10.1016/j.matdes.2015.10.013.
[16] L. Zoli, A. Vinci, P. Galizia, C. Melandri, D. Sciti, On the thermal shock resistance and mechanical properties of novel unidirectional UHTCMCs for extreme environments, Sci. Rep. 8 (2018) 9148, https://doi.org/10.1038/s41598-018-27328-x.
[17] M.X. Shi, B. Liu, Z.Q. Zhang, Y.W. Zhang, H.J. Gao, Direct influence of residual stress on the bending stiffness of cantilever beams, Proc. Math. Phys. Eng. Sci. 468 (2012) 2595–2613, https://doi.org/10.1098/rspa.2011.0662.
[18] A.P. Jackson, J.F.V. Vincent, R.M. Turner, The mechanical design of nacre, Proc. R. Soc. Lond. B Biol. Sci. 234 (1988) 415–440, https://doi.org/10.1098/rspb.1988.0056.
[19] H. Gao, B. Ji, I.L. Jäger, E. Arzt, P. Fratzl, Materials become insensitive to flaws at nanoscale: lessons from nature, Proc. Natl. Acad. Sci. USA 100 (2003) 5597–5600, https://doi.org/10.1073/pnas.0631609100.
[20] P. Fratzl, R. Weinkamer, Nature's hierarchical materials, Prog. Mater. Sci. 52 (2007) 1263–1334, https://doi.org/10.1016/j.pmatsci.2007.06.001.
[21] M.A. Meyers, A.Y.-M. Lin, P.-Y. Chen, J. Muyco, Mechanical strength of abalone nacre: role of the soft organic layer, J. Mech. Behav. Biomed. Mater. 1 (2008) 76–85, https://doi.org/10.1016/j.jmbbm.2007.03.001.
[22] A.Y.-M. Lin, M.A. Meyers, Interfacial shear strength in abalone nacre, J. Mech. Behav. Biomed. Mater. 2 (2009) 607–612, https://doi.org/10.1016/j.jmbbm.2009.04.003.
[23] H.S. Gupta, S. Krauss, M. Kerschnitzki, A. Karunaratne, J.W.C. Dunlop, A. H. Barber, P. Boesecke, S.S. Funari, P. Fratzl, Intrafibrillar plasticity through mineral/collagen sliding is the dominant mechanism for the extreme toughness of antler bone, J. Mech. Behav. Biomed. Mater. 28 (2013) 366–382, https://doi.org/10.1016/j.jmbbm.2013.03.020.